Scientia Iranica, Vol. 15, No. 1, pp 94 107

SCIENTIA IRANICA

Internal Force Tuning of Cooperative Object Manipulation Tasks

R. Rastegari[1] and S.A.A. Moosavian[*]

To manipulate an object with several cooperating manipulators, the Multiple Impedance Control (MIC) is a model-based algorithm that enforces designated impedance on all cooperating manipulators and the manipulated object. For tuning the inner object forces, it is needed to model the inner forces/torques and include them in the MIC law. In this paper, a virtual linkage model is introduced to determine the inner forces in the MIC law. Also, open loop and a closed loop controllers are designed for inner forces tuning. The MIC law will be compared to the relevant algorithms, i.e., Object Impedance Control (OIC) and Augmented Object Control (AOC). Next, the MIC is used to manipulate an object on a planned path with desired inner forces. The grasp condition is considered either solidly (with all cooperating end-effectors), or, as flexible. Finally, the effects of gain tuning on the variations of inner forces will be discussed. The obtained results reveal the merits of the proposed scheme, in terms of system flexibility and good tracking errors, as well as inner forces tuning, even in the presence of impacts caused by contact with the environment.

INTRODUCTION

In order to control interaction forces and system response during contact tasks, force or impedance control strategies are required. Hybrid position/force control has been the basic strategy of several proposed implementations [1,2]. However, because separate force and position subspaces must be maintained and, as control mode switching must be made at many points during most tasks, hybrid control does not provide an attractive interface. Unexpected situations make these switching decisions even more difficult, i.e., the set of natural constraints may not be easily recognized.

Taking the dynamics of the object into consideration, the mechanics of coordinative manipulation by multiple robotic mechanisms have been discussed [3]. Assuming frictional grasp, a computational procedure is proposed to obtain optimal internal forces. A closed chain formulation in the dynamic control of two cooperative manipulators, with equal degrees of freedom, has also been presented [4]. Different issues in the design of a multi-manipulator control system, an environment for the programming and control of cooperative manipulators, have been discussed [5]. Also, various distributed time-varying feedback control laws have been presented for coordinating the motions of multiple robots to capture and manipulate an object [6-8].

For a single manipulator in dynamic interaction with its environment, impedance control has been proposed, which provides the compliant behavior of the manipulator [9]. Impedance control enforces a relationship between the external force(s)/torque(s), acting on the environment, and the position, velocity and acceleration error of the end-effector. This strategy has been extended for contact tasks involving multiple manipulators [10]. A Cartesian impedance controller has been presented to overcome the main problems encountered in fine manipulation, i.e., the effects of friction (and unmodeled dynamics) on robot performance and the occurrence of singularity conditions [11,12]. The implementation of a combined impedance and force control has been proposed to exert a desired force on the environment and, at the same time, generate a desired relationship between this force and the relative location of the point of interaction (contact), with respect to the commanded

1. *Advanced Robotics and Automated Systems (ARAS) Laboratory, Department of Mechanical Engineering, Khajeh-Nasir Toosi University of Technology, 19 Pardis St., Sadra St., Vanaq Square, Tehran, I.R. Iran.*

*. *Corresponding Author, Advanced Robotics and Automated Systems (ARAS) Laboratory, Department of Mechanical Engineering, Khajeh-Nasir Toosi University of Technology, 19 Pardis St., Sadra St., Vanaq Square, Tehran, I.R. Iran.*

manipulator location [13]. Using an exact model of the manipulator, an algorithm is developed, based on feedback and feedforward control theories. Adaptive schemes have also been presented to make impedance control capable of tracking a desired contact force, which has been described as the main shortcoming of impedance control in an unknown environment [14-16].

Object Impedance Control (OIC), an extension of impedance control, has been developed for robotic arms manipulating a common object [17]. The OIC enforces designated impedance, not of an individual manipulator endpoint, but of the manipulated object itself. A combination of feedforward and feedback controls is employed to make the object behave like reference impedance. It has been realized that applying the OIC to a manipulation task of a flexible object may lead to instability [18]. Based on the analysis of a representative system, it was suggested that, in order to solve the instability problem, one should either increase the desired mass parameters or filter and lower the frequency content of the estimated contact force. Internal force control is often applied to compensate for kinematics errors and dynamic interaction forces, for multiple arm coordination. In grasping an object, internal forces must be controlled to satisfy friction constraints and prevent any slippage. In [19], based on a physical representation, a model of internal forces is proposed, which provides a realistic characterization of these forces.

The Multiple Impedance Control (MIC) has been developed for several cooperating arms manipulating an object [20]. The MIC enforces a reference impedance on both the manipulator end-points and the manipulated object. This means that both the manipulator end-effectors and the object are controlled to behave like designated impedance in reaction to any disturbing external force on the object. Hence, an accordant motion of the manipulators and payload is achieved. Besides, an object's inertia effects are compensated for in the impedance law and, at the same time, the end-effectors tracking errors are controlled. The MIC algorithm can also be applied to space robotic systems, in which the manipulators are mounted on a free-flying base [21] or on wheeled robotic systems [22]. In these cases, the formulation is adapted to consider the dynamic coupling between the arms and the base, while the manipulated object may also include an internal source of angular momentum. Under the MIC law, all participating manipulators, the mobile base and the manipulated object exhibit the same impedance behavior, as implied by the name "multiple". A non-model-based version of this algorithm has recently been developed [23], which does not need any information about the system dynamics. Also, the virtual object grasp linkage has been proposed, in order to control the inner object forces in case the MIC law is applied [24].

In this paper, first, the motion equations of a cooperative robotic system, which includes three arms to manipulate a common object in two cases of solid and flexible grasps, are derived. It should be noted that, in the case of using large gains for reaching good tracking, flexibility at the grasp point (that is provided by the Remote Compliance Centre (RCC)) is required, in order to reduce the amount of contact force. The virtual object grasp linkage is introduced and is used to control the inner object forces. To this end, two open-loop and closed-loop controllers are proposed. Then, a conceptual comparison between the MIC law and other relevant algorithms, i.e., Object Impedance Control (OIC) and Augmented Object Control (AOC), will be presented. Finally, the MIC law is applied to three cooperative manipulators, which move a common object. The various capabilities of this controller, in a free motion of the object, also dealing with contact, are examined and the obtained results are discussed. These results reveal good tracking performance and system flexibility, as well as inner forces tuning, even in the presence of impacts due to contact with the environment.

DYNAMICS MODELING

The dynamics of each participating manipulator can be obtained and expressed in the joint space as follows:

$$H^{(i)}\left(q^{(i)}\right).\ddot{q}^{(i)} + C_v^{(i)}\left(q^{(i)}, \dot{q}^{(i)}\right) = Q^{(i)}, \tag{1}$$

where the superscript i corresponds to the ith manipulator and $q^{(i)}$ is the vector of generalized coordinates (consisting of joint angles and displacements). Note that $H^{(i)}$ is the ith manipulator mass matrix and $C_v^{(i)}$ contains all the gravity and nonlinear velocity terms. The vector of generalized forces, $Q^{(i)}$, can be written as follows:

$$Q^{(i)} = Q^{(i)}_{\text{app}} + Q^{(i)}_{\text{react}} + Q^{(i)}_{\text{dist.}}, \tag{2}$$

where $Q^{(i)}_{\text{react}}$ is the effect of the reaction load on the ith end-effector, $Q^{(i)}_{\text{dist}}$ is the effect of disturbance and $Q^{(i)}_{\text{app}}$ is the applied controlling force, which is divided into two parts, motion-concerned and force- concerned as follows:

$$Q^{(i)}_{\text{app}} = Q^{(i)}_m + Q^{(i)}_f, \tag{3}$$

where $Q^{(i)}_m$ is the applied control force causing the motion of the end-effector, while $Q^{(i)}_f$ is the required force to compensate the reaction load effects.

Next, two various grasp conditions, i.e., rigid and flexible, will be discussed.

Rigid Grasp

Ignoring the constraints, the system Degrees Of Freedom (DOF), including n manipulators and the object is as follows:

$$L = \sum_{i=1}^{n} \text{dof}_i + 6, \tag{4}$$

where dof_i is the ith manipulator DOF. The desired motion of the object can be tracked, if the closed chain of robotic arms contains six DOF or more. By taking the constraints into account, the total DOF, i.e. L, is reduced to $(L \quad m)$, where m is the number of grasp constraints that are described as kinematics equations. Therefore, it is necessary to add the kinematics constraint equations to the free-motion equations of the object and the manipulators. To do this, one needs to multiply each kinematics constraint with a Lagrange multiplier and, then, add these terms to the free motion equations [25]. Therefore, the number of equations becomes $L + m$, where m is the number of grasp constraints. Obviously, the number of variables that must be determined is $L + m$, i.e., L variables plus m Lagrange multipliers. It should be noted that the number of independent variables is $L \quad m$, which is equal to the DOF of the constrained system. Therefore, by developing an independent set of dynamics equations, based on recognizing a set of independent variables, or by means of methods like the Natural Orthogonal Complement Method, the computation cost will be reduced [26]. It is by solving these equations that the motion characteristics of the constrained robotic system will be determined.

As shown in Figure 1, the robotic system that manipulates an object in planar motion has three DOF,

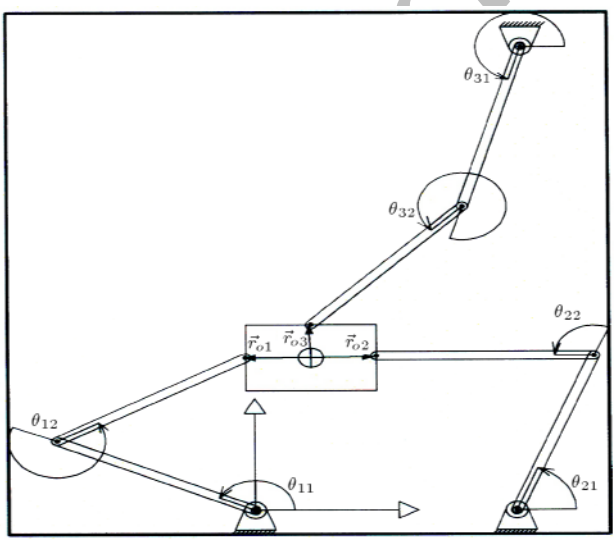

Figure 1. Manipulation of an object with three arms, each with two DOF.

so the number of dynamics equations can be reduced to 3, in terms of 3 independent variables. Then, to determine other variables, one can use the kinematics equations. As can be seen, three planar robots, each with two DOF, have grabbed the object under a point grasp condition. Point grasp means that, at the grasp, a pivoted joint can be substituted. The grasp positions, with respect to the object mass center, are shown in Figure 1 as $\vec{r}_{o1}$, $\vec{r}_{o2}$ and $\vec{r}_{o3}$, where the angles of these vectors, with respect to the object main direction, are 180°, 0°and 90°, respectively. For each grasp, two kinematics constraints can be defined as follows:

$$l_{11}.\begin{Bmatrix}\cos(\theta_{11})\\ \sin(\theta_{11})\end{Bmatrix} + l_{12}.\begin{Bmatrix}\cos(\theta_{11}+\theta_{12})\\ \sin(\theta_{11}+\theta_{12})\end{Bmatrix} = \begin{Bmatrix}x_{obj}\\ y_{obj}\end{Bmatrix} \quad r_{o1}.\begin{Bmatrix}\cos(\varphi)\\ \sin(\varphi)\end{Bmatrix}, \tag{5}$$

where l_{ij} and θ_{ij} represent the length and joint angle of the jth link of the ith manipulator, φ is the object angle, with respect to the inertial coordinate, and x_{obj} and y_{obj} represent the object mass center position. Similarly, for the other two robots, the following can be obtained:

$$\begin{Bmatrix}x_{obj}\\ y_{obj}\end{Bmatrix} + r_{o2}.\begin{Bmatrix}\cos(\varphi)\\ \sin(\varphi)\end{Bmatrix} = \begin{Bmatrix}1.2\\ 0\end{Bmatrix} + l_{21}.\begin{Bmatrix}\cos(\theta_{21})\\ \sin(\theta_{21})\end{Bmatrix} + l_{22}.\begin{Bmatrix}\cos(\theta_{21}+\theta_{22})\\ \sin(\theta_{21}+\theta_{22})\end{Bmatrix}, \tag{6}$$

$$\begin{Bmatrix}x_{obj}\\ y_{obj}\end{Bmatrix} + r_{o3}.\begin{Bmatrix}\sin(\varphi)\\ \cos(\varphi)\end{Bmatrix} = \begin{Bmatrix}1.23\\ 2.8\end{Bmatrix} + l_{31}.\begin{Bmatrix}\cos(\theta_{31})\\ \sin(\theta_{31})\end{Bmatrix} + l_{32}.\begin{Bmatrix}\cos(\theta_{31}+\theta_{31})\\ \sin(\theta_{31}+\theta_{31})\end{Bmatrix}. \tag{7}$$

By taking the variation of these six constraints, the following equation can be obtained:

$$\begin{bmatrix} a_{11} & a_{21} & 0 & 0 & 0 & 0 & a_{31} & a_{41} & a_{51}\\ a_{12} & a_{22} & 0 & 0 & 0 & 0 & a_{32} & a_{42} & a_{52}\\ 0 & 0 & b_{11} & b_{21} & 0 & 0 & b_{31} & b_{41} & b_{51}\\ 0 & 0 & b_{12} & b_{22} & 0 & 0 & b_{32} & b_{42} & b_{52}\\ 0 & 0 & 0 & 0 & c_{11} & c_{21} & c_{31} & c_{41} & c_{51}\\ 0 & 0 & 0 & 0 & c_{12} & c_{22} & c_{32} & c_{42} & c_{52}\end{bmatrix}$$

$$\begin{Bmatrix}\delta\theta_{11}\\ \delta\theta_{12}\\ \delta\theta_{21}\\ \delta\theta_{22}\\ \delta\theta_{31}\\ \delta\theta_{32}\\ \delta x_{obj}\\ \delta y_{obj}\\ \delta\varphi\end{Bmatrix} = \vec{0}. \tag{8}$$

The free motion equations of three planar robots are determined by Equation 1 and the object motion equations can be described as follows:

$$m_{obj}.\ddot{\vec{r}}_{obj} = \vec{f}_o + \vec{f}_c, \tag{9}$$

$$I_{obj}.\ddot{\varphi} = \vec{r}_o \times \vec{f}_o + \vec{r}_c \times \vec{f}_c + \vec{n}_o + \vec{n}_c, \tag{10}$$

where m_{obj} is the object mass, I_o is the mass moment of inertia about the normal axis of the planar plane and $\vec{r}_{obj}$ is the position vector of the object mass center, with respect to the inertial coordinate; $\vec{f}_o$ and $\vec{f}_c$ are the external and the contact forces, respectively, $\vec{n}_o$ is the external torque and $\vec{n}_c$is the contact torque applied on the object; $\vec{r}_o$ is the position vector of the external force and, finally, $\vec{r}_c$ is the position vector of the contact force, with respect to the object center mass. By multiplying each of these equations with a Lagrange multiplier and adding the resulting terms to free motion equations, the constrained motion equations of the robotic system can be obtained. To this end, the following parameters are defined:

$$C_{22} = \begin{bmatrix} c_{31} & c_{32} \\ c_{41} & c_{42} \end{bmatrix}, \qquad B_{22} = \begin{bmatrix} b_{31} & b_{32} \\ b_{41} & b_{42} \end{bmatrix},$$

$$A_{22} = \begin{bmatrix} a_{31} & a_{32} \\ a_{41} & a_{42} \end{bmatrix}, \tag{11}$$

$$G_{22} = \begin{bmatrix} c_{11} & c_{12} \\ c_{21} & c_{22} \end{bmatrix}, \qquad F_{22} = \begin{bmatrix} b_{11} & b_{12} \\ b_{21} & b_{22} \end{bmatrix},$$

$$E_{22} = \begin{bmatrix} a_{11} & a_{12} \\ a_{21} & a_{22} \end{bmatrix}, \tag{12}$$

$$C_{12} = \begin{bmatrix} c_{51} & c_{52} \end{bmatrix}, \qquad B_{12} = \begin{bmatrix} b_{51} & b_{52} \end{bmatrix},$$

$$A_{12} = \begin{bmatrix} a_{51} & a_{52} \end{bmatrix}, \tag{13}$$

$$\vec{\lambda}_i = \begin{Bmatrix} \lambda_{ij} \\ \lambda_{ij} \end{Bmatrix}, \tag{14}$$

where $\vec{\lambda}_i$ contains Lagrange multipliers corresponding to the ith manipulator. Then, the dynamics equations of the constrained robotic system are derived as follows:

$$H_1.\ddot{\vec{q}}_1 + C_{v1} = Q_{\text{app1}} + E_{22}.\vec{\lambda}_1, \tag{15a}$$

$$H_2.\ddot{\vec{q}}_2 + C_{v2} = Q_{\text{app2}} + F_{22}.\vec{\lambda}_2, \tag{15b}$$

$$H_3.\ddot{\vec{q}}_3 + C_{v3} = Q_{\text{app3}} + G_{22}.\vec{\lambda}_3, \tag{15c}$$

$$m_{obj}.\ddot{\vec{r}}_{obj} = \vec{f}_o + \vec{f}_c + A_{22}.\vec{\lambda}_1 + B_{22}.\vec{\lambda}_2 + C_{22}.\vec{\lambda}_3, \tag{15d}$$

$$I_{obj}.\ddot{\varphi} = \vec{r}_o \times \vec{f}_o + \vec{r}_c \times \vec{f}_c + \vec{n}_o + \vec{n}_c + A_{12}.\vec{\lambda}_1 + B_{12}.\vec{\lambda}_2 + C_{12}.\vec{\lambda}_3. \tag{15e}$$

Second differentiation of Equations 5 to 7 yields the acceleration kinematics equations as follows:

$$J_1.\ddot{\vec{q}}_1 = \dot{J}_1.\dot{\vec{q}}_1 + \ddot{\vec{r}}_{obj} + r_{o1}.\begin{Bmatrix} \cos(\varphi) \\ \sin(\varphi) \end{Bmatrix}.\dot{\varphi}^2 - r_{o1}.\begin{Bmatrix} \sin(\varphi) \\ \cos(\varphi) \end{Bmatrix}.\ddot{\varphi}, \tag{16a}$$

$$J_2.\ddot{\vec{q}}_2 = \dot{J}_2.\dot{\vec{q}}_2 + \ddot{\vec{r}}_{obj} + r_{o2}.\begin{Bmatrix} \cos(\varphi) \\ \sin(\varphi) \end{Bmatrix}.\dot{\varphi}^2 - r_{o2}.\begin{Bmatrix} \sin(\varphi) \\ \cos(\varphi) \end{Bmatrix}.\ddot{\varphi}, \tag{16b}$$

$$J_3.\ddot{\vec{q}}_3 = \dot{J}_3.\dot{\vec{q}}_3 + \ddot{\vec{r}}_{obj} + r_{o2}.\begin{Bmatrix} \sin(\varphi) \\ \cos(\varphi) \end{Bmatrix}.\dot{\varphi}^2 - r_{o3}.\begin{Bmatrix} \cos(\varphi) \\ \sin(\varphi) \end{Bmatrix}.\ddot{\varphi}, \tag{16c}$$

where:

$$\vec{q}_i = \begin{Bmatrix} \theta_{i1} \\ \theta_{i2} \end{Bmatrix}. \tag{16d}$$

Equations 15 and 16 make a system of 15 equations with 15 unknown variables, which can be solved to determine the unknown variables. The constrained system has three DOF; so we can reduce the fifteen motion equations to three dynamic motion equations, in terms of $\ddot{\vec{q}}_1$ and $\ddot{\varphi}$ as three independent variables:

$$\begin{bmatrix} K_{11} & K_{12} \\ K_{21} & K_{22} \end{bmatrix}.\begin{Bmatrix} \ddot{\vec{q}}_1 \\ \ddot{\varphi} \end{Bmatrix} = \begin{Bmatrix} V_1 \\ V_2 \end{Bmatrix}, \tag{17a}$$

where:

$$K_{11} = m_{obj}.J_1 \quad A_{22}.{E_{22}}^{1}.H_1 \quad B_{22}.{F_{22}}^{1}.H_2.{J_2}^{1}.J_1 \quad C_{22}.{G_{22}}^{1}.H_3.{J_3}^{1}.J_1, \tag{17b}$$

$$K_{12} = m_{obj}.r_{o1}.\begin{Bmatrix} \sin\varphi \\ \cos\varphi \end{Bmatrix} \quad B_{22}.{F_{22}}^{1}.H_2.{J_2}^{1} .(r_{o1}+r_{o2}).\begin{Bmatrix} \sin\varphi \\ \cos\varphi \end{Bmatrix} \quad C_{22}.{G_{22}}^{1}.H_3.{J_3}^{1} .\left(r_{o1}\begin{Bmatrix} \sin\varphi \\ \cos\varphi \end{Bmatrix} \quad r_{o3}.\begin{Bmatrix} \cos\varphi \\ \sin\varphi \end{Bmatrix}\right), \tag{17c}$$

$$K_{21} = A_{12}.{E_{22}}^{1}.H_1 \quad B_{12}.{F_{22}}^{1}.H_2.{J_2}^{1}.J_1 \quad C_{12}.{G_{22}}^{1}.H_3.{J_3}^{1}.J_1, \tag{17d}$$

$$K_{22} = I_o \quad B_{12}.F_{22}{}^{1}.H_2.J_2{}^{1}.(r_{o1}+r_{o2}).\begin{Bmatrix}\sin\varphi\\ \cos\varphi\end{Bmatrix} \quad C_{12}.G_{22}{}^{1}.H_3.J_3{}^{1}\left(r_{o1}\begin{Bmatrix}\sin\varphi\\ \cos\varphi\end{Bmatrix} \quad r_{o3}.\begin{Bmatrix}\cos\varphi\\ \sin\varphi\end{Bmatrix}\right). \tag{17e}$$

The right hand side of Equation 17a is defined as follows:

$$V_1 = \quad m_{obj}.\left(\dot{J}_1.\dot{\vec{q}}_1 \quad r_{o1}.\begin{Bmatrix}\cos\varphi\\ \sin\varphi\end{Bmatrix}.\dot{\varphi}^2\right)+\vec{f}_o+\vec{f}_c + A_{22}.E_{22}{}^{1}(C_{v1} \quad Q_{\text{app1}})+B_{22}.F_{22}{}^{1}.\left(H_2.J_2{}^{1}.\left(\dot{J}_2.\dot{\vec{q}}_2+\dot{J}_1.\dot{\vec{q}}_1(r_{o1}+r_{o2}).\begin{Bmatrix}\cos\varphi\\ \sin\varphi\end{Bmatrix}.\dot{\varphi}^2\right)+C_{v2} \quad Q_{\text{app2}}\right)+C_{22}.G_{22}{}^{1}.\left(H_3.J_3{}^{1}.\left(\dot{J}_3.\dot{\vec{q}}_3+J_1.\dot{\vec{q}}_1 \quad \left(r_{o1}\begin{Bmatrix}\cos\varphi\\ \sin\varphi\end{Bmatrix} \quad r_{o3}.\begin{Bmatrix}\sin\varphi\\ \cos\varphi\end{Bmatrix}\right).\dot{\varphi}^2\right)+C_{v3} \quad Q_{\text{app3}}\right), \tag{18a}$$

$$V_2 = m_c+n_o+(\vec{r}_o\times\vec{f}_o).\hat{k}+A_{12}.E_{22}{}^{1}(C_{v1} \quad Q_{\text{app1}}) + B_{12}.F_{22}{}^{1}.\left(H_2.J_2{}^{1}.\left(\dot{J}_2.\dot{\vec{q}}_2+\dot{J}_1.\dot{\vec{q}}_1(r_{o1}+r_{o2}).\begin{Bmatrix}\cos\varphi\\ \sin\varphi\end{Bmatrix}.\dot{\varphi}^2\right)+C_{v2} \quad Q_{\text{app2}}\right)+C_{12}.G_{22}{}^{1}.\left(H_3.J_3{}^{1}.\left(\dot{J}_3.\dot{\vec{q}}_3+\dot{J}_1.\dot{\vec{q}}_1 \quad \left(r_{o1}\begin{Bmatrix}\cos\varphi\\ \sin\varphi\end{Bmatrix} \quad r_{o3}.\begin{Bmatrix}\sin\varphi\\ \cos\varphi\end{Bmatrix}\right).\dot{\varphi}^2\right)+C_{v3} \quad Q_{\text{app3}}\right). \tag{18b}$$

Form the kinematics Equations 16, one can obtain $\ddot{\vec{q}}_2$ and $\ddot{\vec{q}}_3$ for the other two manipulators as follows:

$$\ddot{\vec{q}}_2 = J_2{}^{1}.\left(\dot{J}_2.\dot{\vec{q}}_2+\dot{J}_1.\dot{\vec{q}}_1 \quad (r_{o1}+r_{o2}).\begin{Bmatrix}\cos\varphi\\ \sin\varphi\end{Bmatrix}.\dot{\varphi}^2 + J_1.\ddot{\vec{q}}_1+(r_{o1}+r_{o2}).\begin{Bmatrix}\sin\varphi\\ \cos\varphi\end{Bmatrix}.\ddot{\varphi}\right), \tag{19a}$$

$$\ddot{\vec{q}}_3 = J_3{}^{1}.\left(\dot{J}_3.\dot{\vec{q}}_3+\dot{J}_1.\dot{\vec{q}}_1 \quad \left(r_{o1}.\begin{Bmatrix}\cos\varphi\\ \sin\varphi\end{Bmatrix} \quad r_{o3}.\begin{Bmatrix}\sin\varphi\\ \cos\varphi\end{Bmatrix}\right).\dot{\varphi}^2+J_1.\ddot{\vec{q}}_1+\left(r_{o1}\begin{Bmatrix}\sin\varphi\\ \cos\varphi\end{Bmatrix} \quad r_{o3}\begin{Bmatrix}\cos\varphi\\ \sin\varphi\end{Bmatrix}\right).\ddot{\varphi}\right). \tag{19b}$$

Therefore, Equations 17 will be solved first and, then, by substituting the results into Equations 19, the variables of the other two manipulators can be obtained. Also, the Lagrange multipliers are obtained from Equations 15. Next, the applied forces exerted by the end-effectors on the object are derived as follows:

$$\vec{f}_{s3}=C_{22}.\vec{\lambda}_3, \qquad \vec{f}_{s2}=B_{22}.\vec{\lambda}_2, \qquad \vec{f}_{s1}=A_{22}.\vec{\lambda}_1. \tag{20}$$

Flexible Grasp

The existence of flexibility in the grasp helps to accomplish a manipulation task securely [27]. Besides, usually, some flexibility exists in the system, for instance, at the robot joints, links and in the object itself. Here, it is assumed that the flexibility of the system is concentrated at the grasp point, as provided by the Remote Compliance Centre, RCC. The motion dynamics of cooperative robots with such flexible elements that an object can be moved, is to be derived. To this end, Equation 1 will describe the motion equations of the cooperative manipulators. At each grasp point, where a flexible element exists, the corresponding kinematics equations, described in Equations 5 to 7, are omitted. Instead, the flexible element relates the motion of the end-effector and the manipulated object. In other words, the kinematics constraints should only be considered at the rigid grasp points. Therefore, by solving the resulting equations, the robotic system behavior and the manipulated object will be determined.

MIC LAW AND INTERNAL FORCE ADJUSTMENT

In this section, first, a brief description of the MIC law is introduced. Next, a model of the object internal forces is developed, which relates the inner object forces and the end-effectors applied forces. Then, the developed model is used, by the MIC law, in order to control the object inner forces and moments. Finally, two basic approaches, which consist of open and closed loop controllers, are proposed, for tuning the inner forces and moments.

Multiple Impedance Control Law

The MIC enforces a reference impedance on both the manipulator end-points and the manipulated object. This means that both manipulator end-effectors and the object are controlled to behave like a designated impedance in reaction to any disturbing external force on the object. Hence, an accordant motion of the manipulators and payload is achieved. Besides, an object's inertia effects are compensated for by the impedance law and, at the same time, the end-effector(s) tracking errors are controlled. The applied force in MIC consists of virtually two separate parts that are concerned with the motion of the end-effectors, $\tilde{Q}_m^{(i)}$, and the force to be exerted on the object, $\tilde{Q}_f^{(i)}$. More precisely, the motion part determines the forces required to make the end-effectors follow their desired path and the force part compensates for the manipulated object reaction forces exerted on the end-effectors. The applied motion forces are obtained, based on a feedback linearization scheme as follows [20]:

$$\tilde{Q}_m^{(i)} = \tilde{H}^{(i)} \tilde{M}_{\text{des}}^{-1} \cdot \left[\tilde{M}_{\text{des}} . \ddot{\tilde{x}}_{\text{des}}^{(i)} + \tilde{K}_d . \dot{\tilde{e}}^{(i)} + \tilde{K}_p . \tilde{e}^{(i)} + F_c \right] + \tilde{C}^{(i)}, \tag{21}$$

where $\tilde{M}_{\text{des}}$, $\tilde{K}_d$ and $\tilde{K}_p$ are mass, damping and stiffness gain matrices, respectively. The applied force commands can be obtained, based on applying an impedance law to the object motion as follows [20]:

$$G.F_{\text{des}} = M M_{\text{des}}^{-1} (M_{\text{des}} \ddot{x}_{\text{des}} + K_d \dot{e} + K_p e + F_c) + F_\omega \quad (F_c + F_o), \tag{22}$$

where M_{des}, K_d and K_P are mass, damping and stiffness gain matrices of applied impedance on an object, respectively, and G is the grasp matrix. A quasi-static model, to determine the object inner forces and moments, has been proposed in [19]. By combining this model and the force command in the MIC law, one can relate the end-effector forces/moments to the resultant object force/moment, with a non-singular, full rank matrix, W as follows:

$$\begin{Bmatrix} \vec{f}_r \\ \vec{m}_r \\ \vec{t} \\ \vec{\tau} \end{Bmatrix} = W.F_{\text{des}}, \qquad W = \begin{bmatrix} G \\ \hat{E} \end{bmatrix}_{12\times 12}, \tag{23}$$

where $\vec{f}_r$ expresses the motion force command, $\vec{m}_r$ is the motion torque command, $\vec{t}$ and $\vec{\tau}$ are the inner forces and torques, respectively, and $\hat{E}$ is defined as follows:

$$\begin{Bmatrix} \vec{t} \\ \vec{\tau} \end{Bmatrix} = \hat{E}.F_e, \qquad \hat{E} = \begin{bmatrix} \overline{E}_{3\times 9} & 0_{3\times 9} \\ 0_{9\times 9} & 1_{9\times 9} \end{bmatrix}, \tag{24a}$$

where $\overline{E}$ is a left inverse of E as follows:

$$\overline{E} = \left(E^T.E \right)^{-1} .E^T, \tag{24b}$$

and F_e is obtained as follows:

$$F_e = \begin{Bmatrix} E.\vec{t} + \vec{f}_r \\ m_r \end{Bmatrix}. \tag{24c}$$

By substituting Equation 23 into Equation 9, the force commands applied on cooperative end-effectors in the MIC law are obtained as follows:

$$F_{\text{des}} = W^{-1} . \begin{Bmatrix} \vec{f}_r \\ \vec{m}_r \\ \vec{t} \\ \vec{\tau} \end{Bmatrix}. \tag{25}$$

So, the force part command is determined as follows [20]:

$$\tilde{Q}_f = \begin{Bmatrix} 0_{6\times 1} \\ F_{\text{des}} \end{Bmatrix}. \tag{26}$$

Internal Force Control in MIC

The object path tracking is accomplished by appropriate determination of the motion force command, $\vec{f}_r$, and the motion torque commands, $\vec{m}_r$, in the MIC algorithm. Then, by noting that the grasp matrix, G, is a non-square matrix, the desired internal force and motion are used as follows:

$$F_{\text{des}} = W^{-1} . \begin{Bmatrix} \vec{f}_r \\ \vec{m}_r \\ \vec{t}_{\text{des}} \\ \vec{\tau}_{\text{des}} \end{Bmatrix}. \tag{27}$$

As shown in Figure 2, Equation 27 can be used as an open loop controller to yield the desired force and torque command to be applied on all the cooperative end-effecters that manipulate the object. Also, by considering the advantages of closed-loop controllers, a closed-loop controller can be designed for tuning the internal forces and moments. A P-action controller has been shown in Figure 3.

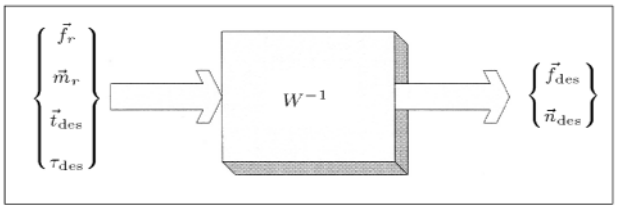

Figure 2. The open loop control of inner forces/moments.

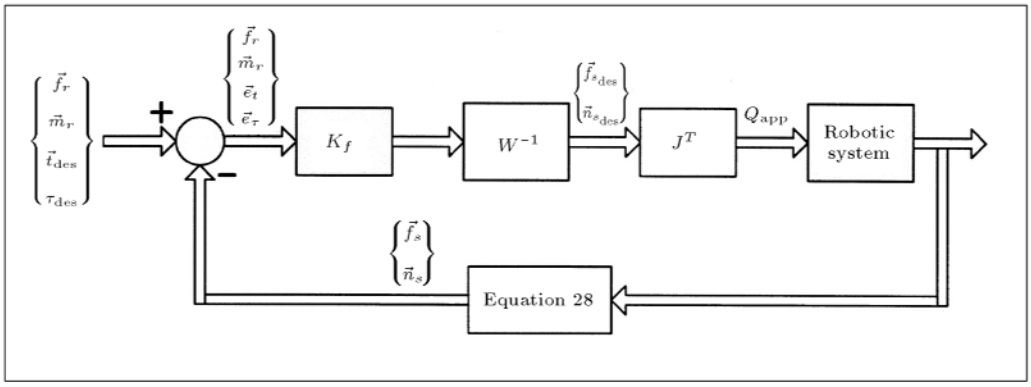

Figure 3. A P-action closed loop control for tuning the inner forces/moments.

CONTROL LAW COMPARISONS

In this section, the Multiple Impedance Control (MIC) is compared structurally with the Object Impedance Control (OIC) and the Augmented Object Control (AOC), where an augmented object model is introduced to the impedance law [24]. All of these three control laws determine the cooperative robots commands to perform an object manipulation task. The OIC law enforces the impedance control law only on the manipulated object. To this end, the desired free motion acceleration of each end-effector is obtained from reflecting the object desired motion acceleration, $\ddot{x}_{\rm cmd}$, to each end-effecter and the free motion command for them as obtained separately [17]. On the other hand, under the MIC law, the impedance control is enforced on the manipulated object and each participating end-effector, including the base platform when dealing with mobile robotic systems [21].

The structural difference between the two methods appears in the presence of flexibility. In this case, the object acceleration reflection of OIC on the cooperative end-effectors is not accurate and the resulting errors, due to flexibility, may even make the system unstable [18]. However, in the MIC law, the free motion commands of the end-effectors are independent from the object motion. Therefore, by applying the MIC law, the system is capable of performing manipulation tasks, even in the presence of flexibility [20,21].

The AOC has a different structure from the two described methods. In this method, the dynamics of a robotic system is projected onto the manipulated object. By applying the impedance control law on such an augmented object, the object and the robotic system have the same behavior, based on the designated impedance control law. The forces/moments commands applied by AOC to cooperative actuators contain both free motions and forces commands. Noting that the forces/moments commands applied to the end-effectors are obtained from the impedance control law, it is clear that the AOC considers the dynamics of the total system. Therefore, in this method, there is no need to reflect $\ddot{x}_{\rm cmd}$ on the end-effectors, as is the case in the OIC law. The AOC law enforces a unique command to all cooperative actuators based on the grasp matrix. Therefore, the AOC can be expected to accomplish the task properly, even in the presence of flexibility, although the existence of flexible elements at the grasp points may cause some errors in executing the desired object tracking task.

The performance of the MIC has been already compared to the OIC [20,21], concluding its greater advantages. Here, the performance of the MIC will be compared to the AOC.

SIMULATION RESULTS AND DISCUSSIONS

System Specifications

In this section, first, the simulation conditions and system parameters are presented. Then, two cases, consisting of solid and flexible grasp conditions, will be considered and the results of applying the MIC and AOC controllers are discussed and compared.

As seen in Figure 1, the cooperative task for object manipulation is performed using three planar robots, each with two DOF, where all links are one meter long. The motions of the manipulators and the object are considered in the horizontal plane. The manipulated object is captured at three contact points, which are located with respect to the object center mass as follows:

$$\vec{r}_{o3} = 0.2\hat{j}, \qquad \vec{r}_{o2} = 0.3\hat{i}, \qquad \vec{r}_{o1} = \quad 0.3\hat{i}.$$

The initial velocity of all joints and the object is zero, while the initial joint variables are obtained accordingly as given in Table 1. The first robot fixed joint is located at the inertial coordinate origin and those of the other robots are located as follows:

$$\vec{R}_{o3} = 1.23i + 2.8\hat{j}, \qquad \vec{R}_{o2} = 1.2\hat{i}.$$

Table 1. The initial joint variables.

θ_{11}	θ_{12}	θ_{21}	θ_{22}	θ_{31}	θ_{32}	φ_{obj}
155°	125°	69.1°	108.6°	254.8°	-31.4°	5.0°

The dynamics parameters of the object and the manipulators are determined as given in Table 2. The saturation limits for actuator torques are given in Table 3.

The desired path is designed as an S-shaped profile, with three independent variables, x and y as translational variables and φ as the orientation variable. It should be mentioned that choosing an S-shaped path makes the control problem more challenging, due to the fact that the desired acceleration direction changes at its inflection point, which works like exerting an impact to the system at that point. The desired orientation is defined to maintain a given direction of the object parallel to the desired velocity vector. An obstacle is considered along the desired path to examine the performance of the algorithm dealing with impacts due to contact. The obstacle stiffness and damping are considered as follows:

$$K_{pw} = 100000 \text{ N/m}, \qquad K_{de} = 5000 \text{ N.sec/m}.$$

The controller gains in applying the MIC law in these simulations are as follows:

$$m_{\text{des}} = 10, \qquad K_p = 3000, \qquad K_d = 600.$$

Next, the MIC law is applied to all three cooperative robotic arms to manipulate an object, as well as tuning the inner forces in the object. As mentioned before, two cases of solid and flexible grasps are simulated separately. These results are, subsequently, compared to those of the AOC law.

Application of the MIC Law with Rigid Grasps

First, the object grasp is established rigidly at all three end-effectors. Figure 4 represents the object tracking path. As seen in Figures 4a and 4b, the object path tracking is properly followed in free motion

Table 2. The dynamics parameters of the object and the manipulators.

m_{i1} [kg]	m_{i2} [kg]	I_{i1} [kgm^2]	I_{i2} [kgm^2]	$m_{obj.}$ [kg]	$I_{obj.}$ [kgm^2]
10	8	1.5	0.8	3	0.5

Table 3. The saturation limits for actuator torques (in N.m).

τ_{11}	τ_{12}	τ_{21}	τ_{22}	τ_{31}	τ_{32}
100	100	100	100	100	100

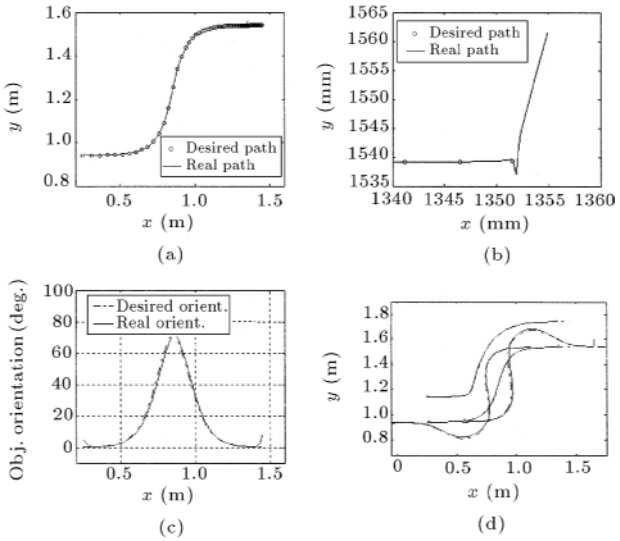

Figure 4. Applying the MIC law to three cooperative arms with rigid grasps and contact; (a) Desired and real object path; (b) Desired and real paths at the contact point; (c) Object orientation trajectory and (d) End-effectors path.

and, when contact with the environment occurs, it smoothly reaches its equilibrium situation. Figure 4c shows the object orientation tracking that follows with small errors, while after contact, it is observed that small steady errors remain in the object orientations. It should be noted that, in free motion, the object tracking errors become more appropriate, by selecting a large gain, but the steady state errors in the y-direction is due to steady state object orientation error (Figure 5). Also, large variations in velocity error happen when the desired acceleration direction changes at the inflection point of the S-shaped path. As seen in Figure 6, the contact force reaches 240 N, because of determining the large proportional gain, $K_P = 3000$. The tracking errors are reduced, but the steady state contact force is increased. The steady state error in object rotation produced y-direction forces in the second and third end-effectors. So, it can be observed that the steady state forces are in a y-direction in the second and third end-effectors. Also, the force equilibrium is observed in the object between the environment contact forces and the end-effectors applied forces.

Application of the MIC Law with Flexible Grasps

In these simulations, the object is grasped by three flexible grasp points, which manipulate the object to track the desired S-shaped path and regulate the inner forces by applying the MIC law. As mentioned before, in case of using large gains for reaching good tracking, flexibility in the grasp condition (that is provided by

a Remote Compliance Centre (RCC)) is required, in order to reduce the amount of contact force. The stiffness and damping specifications of the RCC are considered, with low impedance as follows:

$$K_{pe} = 120 \text{ N/m}, \qquad K_{de} = 50 \text{ N.sec/m}.$$

Figure 7 shows the object inner forces, besides actuator torques, which prepare the object contact forces in contact. As seen in the inner forces diagram, one can observe the steady state errors in the inner forces after contact, because large contact forces are in contact and the actuators have reached saturation conditions due to the rigid grasps.

The simulation results, in cases of flexible grasp, are shown in Figures 8-11. The object and end-effectors path tracking characteristics are shown in Figure 8. As can be seen, the impact appears due to contact with the obstacle, which is deliberately considered in the desired path, to reveal the merits of the proposed scheme. The object error in the y-direction is about 8

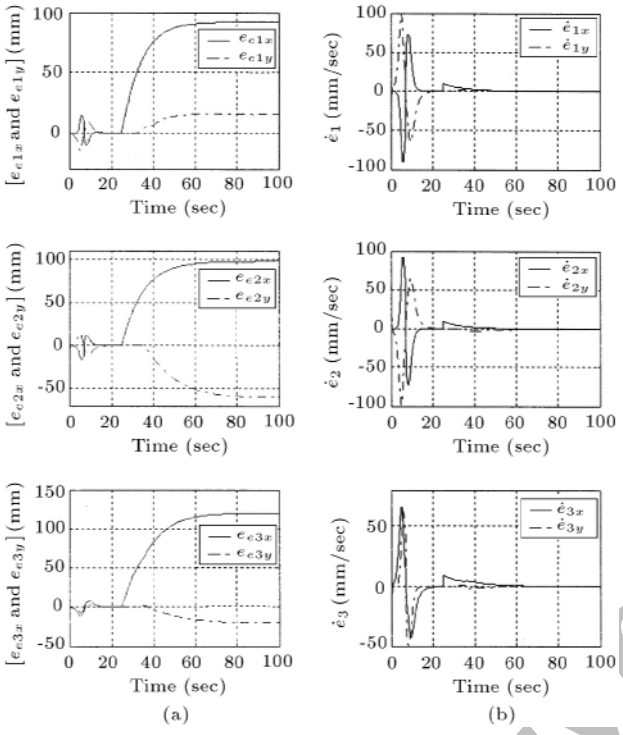

Figure 5. Rigid grasps; a) Tracking errors of the first, second and third end-effectors and b) Corresponding velocity errors.

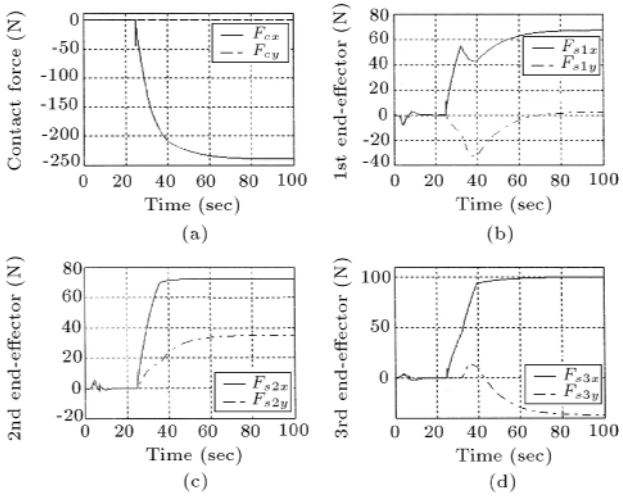

Figure 6. (a) Contact forces history; (b) Applied forces by the first end-effector; (c) Applied forces by the second end-effector and (d) Applied forces by the third end-effector.

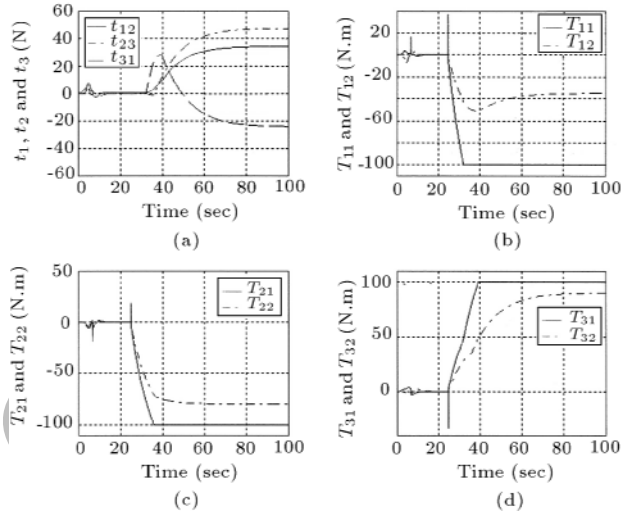

Figure 7. (a) Object inner forces profile; (b) Actuator torques of the first manipulator; (c) Actuator torques of the second manipulator and (d) Actuator torques of the third manipulator.

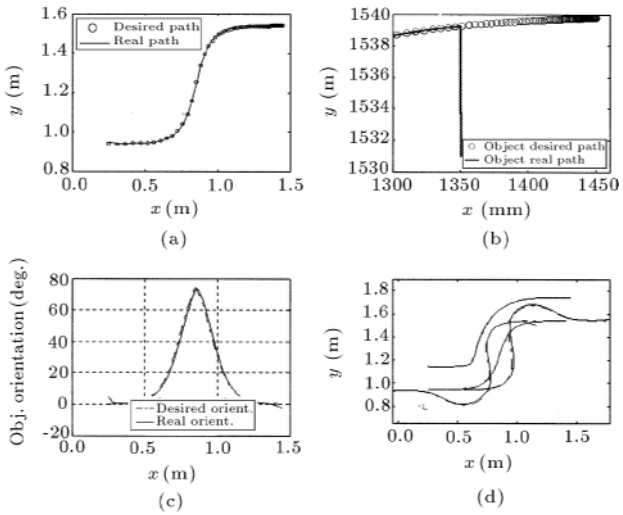

Figure 8. Applying the MIC law to three cooperative end-effectors with flexible grasps and contact; (a) Desired and real object path; (b) Desired and real paths at the contact point; (c) Object orientation trajectory and (d) End-effectors path.

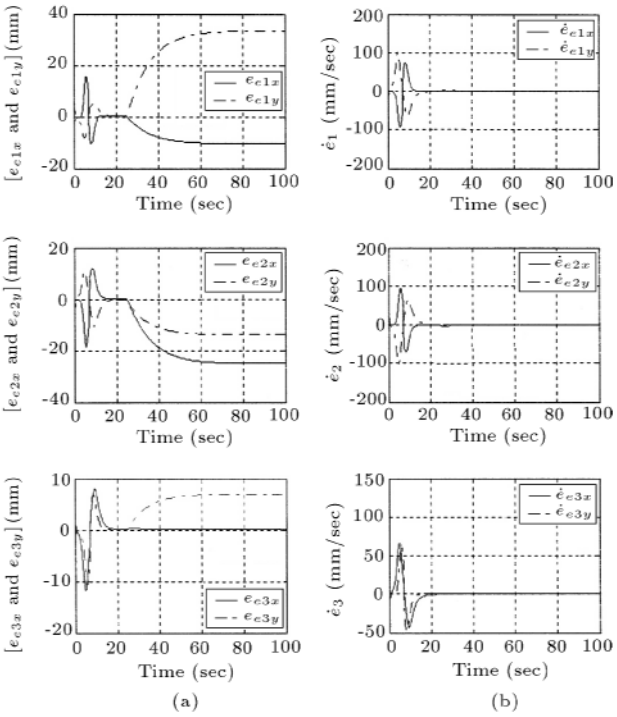

Figure 9. Flexible grasps; a) Tracking errors of the first, second and third end-effectors and b) Corresponding velocity errors.

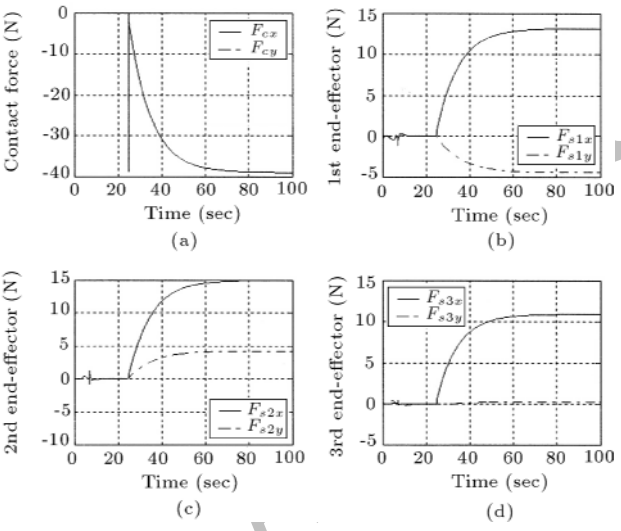

Figure 10. Flexible grasps; (a) Contact forces; (b) Applied forces by the first end-effector; (c) Applied forces by the second end-effector and (d) Applied forces by the third end-effector.

mm and the steady state orientation errors are about 3 degrees. The end-effectors tracking errors and their time rates, before and after contact, are presented in Figure 9.

As seen in Figure 9, tracking errors become considerable in transient response at the inflection point of the S-shaped path and, also, at the time of contact with the obstacle ($t \simeq 25$ S) The contact forces and the

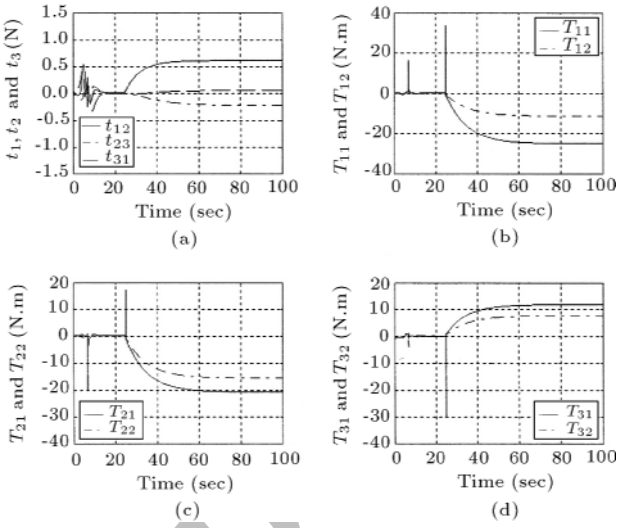

Figure 11. Flexible grasps; (a) Object inner forces error; (b) Actuator torques of the first manipulator; (c) Actuator torques of the second manipulator and (d) Actuator torques of the third manipulator.

exerted end-effectors forces are shown in Figure 10. As can be seen, the MIC is able to manage the contact in a smooth, soft condition. It can be observed that the contact forces and, also, the end-effector exerted forces remain adequately low. In Figure 11, the errors of the object inner forces and the actuator torques are shown. It can be seen that the object inner forces errors are negligible, i.e. a maximum of 0.5 N, and the actuator torques are reasonably within their limits.

Application of the AOC Law with Flexible Grasps

In this section, the recent simulations are repeated by applying the AOC law and the results are shown in Figures 12 to 17. As shown in Figure 12, the object path tracking is performed properly and the end-effectors, also, all properly track their desired path. Figure 13 shows the inner object forces besides the actuator torques.

As seen in Figure 13, the inner forces approach their corresponding desired values, after passing a transient phase at the inflection point of the object path. The maximum variation appears at the inflection point of the path and the errors of the inner forces are much larger (about ten times more) than those obtained by applying the MIC law (Figure 11). Also, at the inflection point, larger actuator torques are demanded, compared to those required by the MIC.

The object tracking errors of applying the AOC law, when a contact with an obstacle has been planned in the desired trajectory, are shown in Figure 14. It can be seen that the object path tracking is obtained, but the behavior of the three end-effectors are out of the

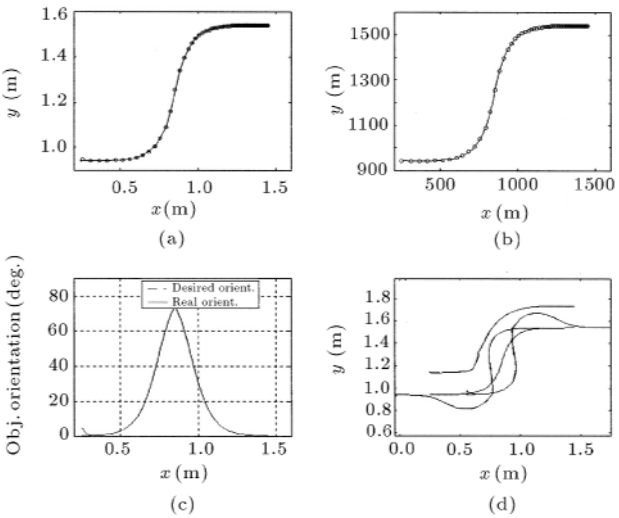

Figure 12. Applying the AOC law to three cooperative end-effectors with flexible grasps without contact; (a) Desired and real object path; (b) Desired and real paths; (c) Object orientation trajectory and (d) End-effectors path.

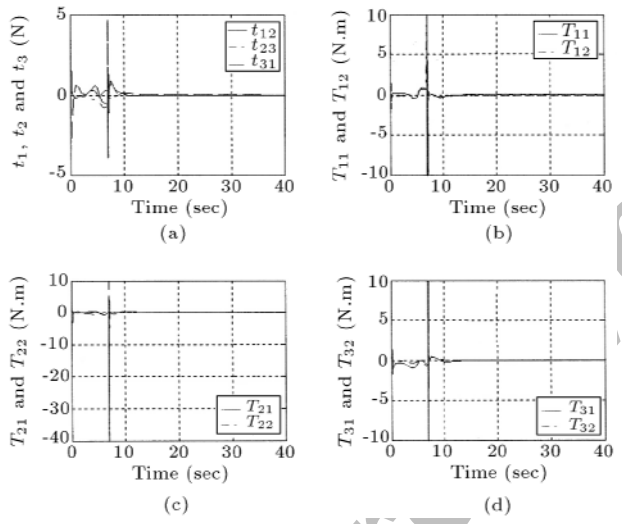

Figure 13. Flexible grasps without contact; (a) Object inner forces error: (b) Actuator torques of the first manipulator; (c) Actuator torques of the second manipulator and (d) Actuator torques of the third manipulator.

ordinary. Due to flexibility, to yield the desired forces, the end-effectors go far away from the object center as shown in Figure 14d.

Tracking and the time rate errors of end-effectors, before and after contact, are presented in Figure 15. Comparing these results to those obtained by applying the MIC (Figure 9), it can be seen that the errors of the AOC are much larger (more than twenty times). Undoubtedly, the reasons for such a difference are in the structural differences between the MIC and AOC laws, as discussed in the previous section. In Figure 16,

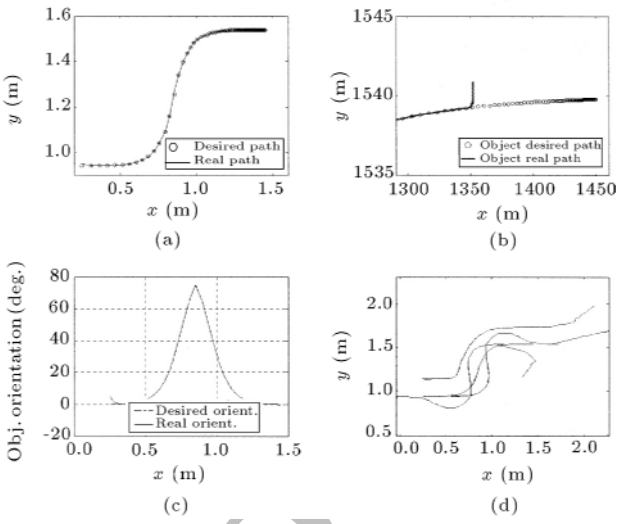

Figure 14. Applying AOC law on three cooperative end-effectors with flexible grasps and contact; (a) Desired and real object path; (b) Desired and real paths at the contact point; (c) Object orientation trajectory and (d) end-effectors path.

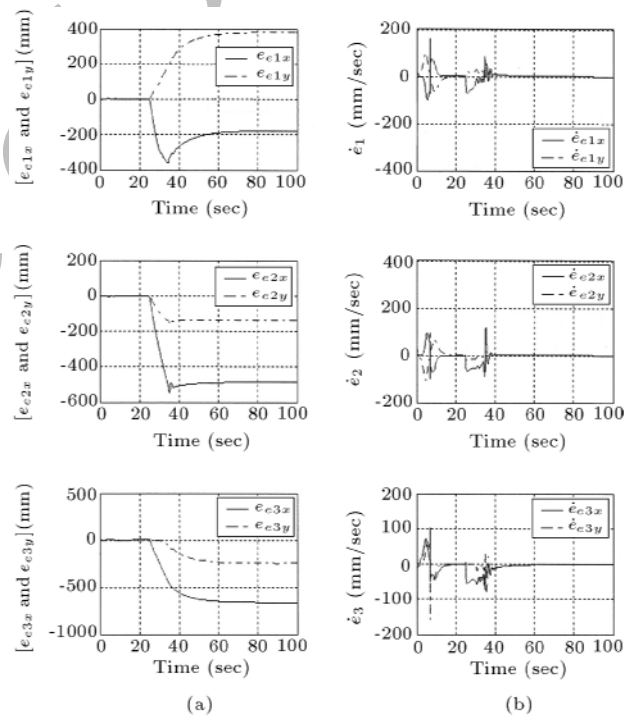

Figure 15. Applying AOC law, flexible grasps with contact; a) Tracking errors of the first, second and third end-effectors and b) Corresponding velocity errors.

it can be seen that the object contact forces are more than five times greater than those obtained by applying the MIC law (Figure 10) and, consequently, so are the applied forces exerted on the object by the end-effectors.

As seen in Figure 17, the object inner forces obtained by applying the AOC law are more than five

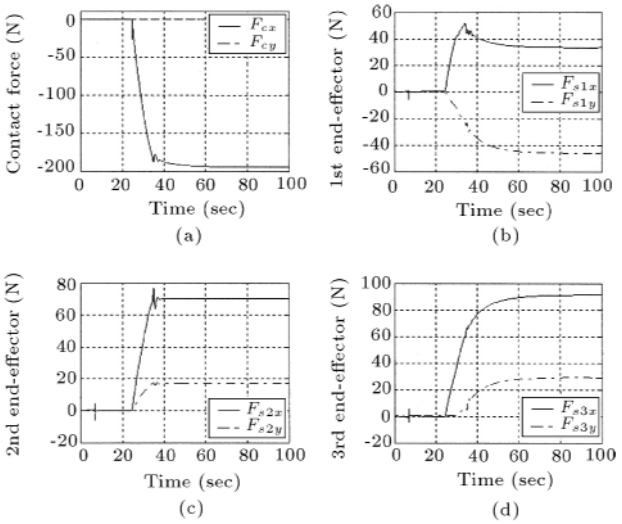

Figure 16. Applying AOC law, flexible grasps with contact; (a) Contact forces; (b) Applying forces by the first end-effector; (c) Applying forces by the second end-effector and (d) Applying forces by the third end-effector.

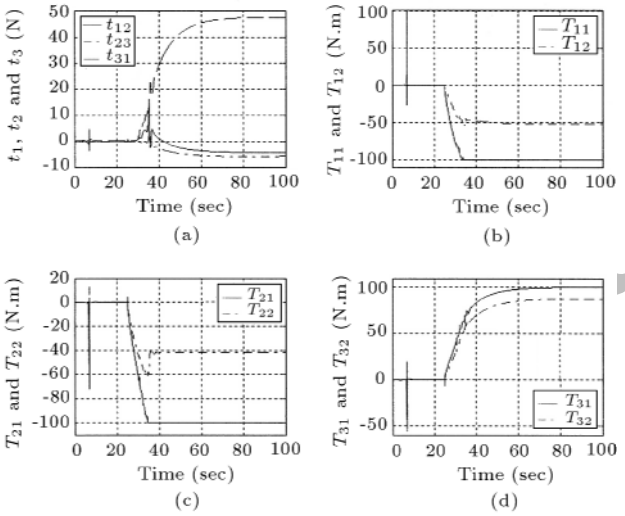

Figure 17. Applying AOC law, flexible grasps with contact; (a) Object inner forces error; (b) Actuator torques of the first manipulator; (c) Actuator torques of the second manipulator and (d) Actuator torques of the third manipulator.

times greater than those corresponding to the MIC (Figure 11). In fact, the flexibility causes deterioration in the AOC performance, which is, in turn, due to errors in projecting the manipulator dynamics on the augmented object model.

These results reveal the merits of the MIC scheme, in terms of system flexibility and good tracking errors, as well as inner forces tuning, even in the presence of impacts, due to contact with the environment. Next, the effects of controller gains tuning on the performance of this algorithm will be briefly detailed.

Study of the Effects of Controller Gains Tuning on the Performance of the MIC

Several cases, such as solid grasp, one flexible grasp and three flexible grasps of three manipulators, have been simulated, to investigate the object inner forces/moments variations along an S-shaped path.

In these simulations, the stiffness controller gain, K_p, is reduced from 3000 to 30, which reflects the various virtual stiffness of cooperative end-effectors and the object in reaction to the environment. As expected, based on physical intuition, all tracking errors are increased, while the behavior of object tracking at the inflection point and at the contact time become smoother. Also, the applied forces from the object to the environment and, consequently, from the end-effectors to the object, are reduced.

Next, the desired mass controller gain, M_{des}, which represents the inertia property of the cooperative robotic manipulators and the object, is increased from 10 to 100. It is observed, by this increase, that the system robustness is increased and the tracking errors at the inflection point and the contact point are reduced.

Finally, the damping controller gain, K_d, is decreased from 600 to 60, in order to observe the inner forces variations. As expected, the effects of contact at its starting time are reduced; therefore, the inner forces in the object are decreased and the overall behavior of the robotic system becomes smoother.

CONCLUSIONS

The inner forces/torques in a manipulated object were modeled using a virtual linkage approach. This approach was used to determine the relationship between the inner forces/torques in the object and the applied forces/ torques, by cooperative end-effectors, under the MIC law. Also, open and closed loop controllers were designed for inner forces tuning. Both the MIC and the AOC laws were implemented to manipulate an object, based on a planned path and desired inner forces. An obstacle was considered along the desired path, to examine the performance of the algorithm dealing with the impacts due to contact. The object was grasped with three cooperating end-effectors, either under solid or flexible conditions. It should be noted that in cases of using large gains for reaching good tracking, that flexibility in the grasp condition (that is provided by a Remote Compliance Centre (RCC)) is required to reduce the amount of contact force. Structural differences between the two methods, MIC and AOC, were discussed. In the AOC method, the commands are projected to any end-effectors by the grasp matrix and, then, to the robotic system actuators. If the flexibility is considerable, the reflection of

the robotic system dynamics on the augmented object may be corrupted. In the MIC law, the desired force commands are applied to the manipulators through a grasp matrix and the free motion commands are determined, by applying the impedance law on each end-effector. Therefore, this algorithm has a good tracking behavior, even in the presence of system flexibility. The other advantage of the MIC law is that it can be applied to mobile robotic systems with a massive base and large accelerations. This is due to this fact that free motion commands are independent from the grasp matrix, but the AOC can only be used for fixed base robots. The simulation results reveal large flexibility at all grasp points and a good tracking performance of the MIC law, as well as inner forces tuning, even in the presence of impact due to contact.

REFERENCES

1. Raibert, M.H. and Craig, J.J. "Hybrid position/force control of manipulators", *ASME Journal of Dynamic Systems, Measurement & Control*, **126**, pp 126-133 (June 1981).
2. Hayati, S. "Hybrid position/force control of multi-arm cooperating robots", *Proc. IEEE Int. Conf. Robotics Automation*, pp 82-89, San Francisco, USA (Apr. 1986).
3. Nakamura, Y., Nagai, K. and Yoshikawa, T. "Mechanics of coordinative manipulation by multiple robotic mechanisms", *Proc. of IEEE Int. Conf. on Robotics and Automation*, pp 991-998 (1987).
4. Tarn, T.J., Bejczy, A.K. and Yun, X. "Design of dynamic control of two cooperating robot arms: Closed chain formulation", *Proc. of IEEE Int. Conf. on Robotics and Automation*, pp 7-13 (1987).
5. Hayward, V. and Hayati, S. "KALI: An environment for the programming and control of cooperative manipulators", *Proc. of American Control Conf.*, pp 473-478, Piscataway, NJ, USA (1988).
6. Yamaguchi, H. "A distributed motion coordination strategy for multiple nonholonomic mobile robots in cooperative hunting operations", *Journal of Robotics and Autonomous Systems*, **43**(4), pp 257-282 (2003).
7. Ahmadabadi, M.N. and Nakano, E. "A constrain and move approach to distributed object manipulation", *IEEE Transactions on Robotics and Automation*, **17**(2), pp 157-172 (April 2001).
8. Yoshikawa, T. and Nagai, K. "Manipulating and grasping forces in manipulation by multifingered robot hands", *IEEE J. of Robotics and Automation*, **7**(1), pp 67-77 (1991).
9. Hogan, N. "Impedance control: An approach to manipulation", *ASME Journal of Dynamic Systems, Measurement & Control*, **107**, pp 1-24 (1985).
10. Caccavale, F. and Villani, L. "An impedance control strategy for cooperative manipulation", *in Proc. of IEEE/ASME Int. Conf. on Advanced Intelligent Mechatronics*, Italy (2001).
11. Biagiotti, L., Liu, H., Hirzinger, G. and Melchiorri, C. "Cartesian impedance control for dexterous manipulation", *in Proc. of IEEE/RSJ Int. Conf. on Intelligent Robots and Systems*, Las Vegas, Nevada, USA (2003).
12. Abiko, S., Lampariello, R. and Hirzinger, G. "Impedance control for a free-floating robot in the grasping of a tumbling target with parameter uncertainty", *Proc. of the IEEE/RSJ Int. Conf. on Intelligent Robots and Systems*, pp 1020-1025, Beijing, China (Oct. 9-15 2006).
13. Goldenberg, A.A. "Implementation of force and impedance control in robot manipulators", *in Proc. of the IEEE Int. Conf. on Robotics and Automation*, pp 1626-1632, Philadelphia, Pennsylvania, USA (1988).
14. Seraji, H. and Colbaugh, R. "Force tracking in impedance control", *Proc. of IEEE Int. Conf. on Robotics and Automation*, pp 499-506, Atlanta, Georgia, USA (1993).
15. Jung, S. and Hsia, T.C. "Stability and convergence analysis of robust adaptive force tracking impedance control of robot manipulators", *Proc. of the IEEE/RSJ Int. Conf. on Intelligent Robots and Systems*, Korea (1999).
16. Ali, S., Moosavian, A. and Rastegari, R. "Multiple-arm space free-flying robots for manipulating objects with force tracking restrictions", *Journal of Robotics and Autonomous Systems*, **54**(10), pp 779-788 (2006).
17. Schneider, S.A. and Cannon, R.H. "Object impedance control for cooperative manipulation: Theory and experimental results", *IEEE Transactions on Robotics and Automation*, **8**(3), pp 383-394 (June 1992).
18. Meer, D.W. and Rock, S.M. "Coupled system stability of flexible-object impedance control", *Proc. of the IEEE Int. Conf. on Robotics and Automation*, pp 1839-1845, Nagoya, Japan (May 1995),
19. Williams, D. and Khatib, O. "The virtual linkage: A model for internal forces in multi-grasp manipulation", *Proc. of the IEEE Int. Conf. Robotics and Automation*, pp 1025-1030 (1993).
20. Ali, S., Moosavian, A. and Papadopoulos, E. "Multiple impedance control for object manipulation", *Proc. of the IEEE/RSJ Int. Conf. on Intelligent Robots and Systems*, Victoria, Canada (Oct. 13-17 1998).
21. Ali, S., Moosavian, A., Rastegari, R. and Papadopoulos, E. "Multiple impedance control for space free-flying robots", *AIAA Journal of Guidance, Control, and Dynamics*, **28**(5), pp 939-947 (Sept. 2005).
22. Rastegari, R., Ali, S. and Moosavian, A. "Multiple impedance control of non-holonomic wheeled mobile robotic systems performing object manipulation tasks", *Journal of Engineering Faculty*, Tehran University, **39**(1), pp 15-30 (May 2005) (written in Persian).

23. Ali, S., Moosavian, A. and Ashtiani, H.R. "Cooperative object manipulation using non-model-based multiple impedance control", *Proc. of the IEEE International Conference on Control Applications (CCA)*, Munich, Germany (Oct. 4-6 2006).

24. Rastegari, R., Ali. S. and Moosavian, A. "Multiple impedance control of cooperative manipulators using virtual object grasp", *Proc. of the IEEE International Conference on Control Applications (CCA)*, Munich, Germany (Oct. 4-6 2006).

25. Meirovitch, L., *Methods of Analytical Dynamics*, McGraw-Hill (1970).

26. Saha, S.K. and Angeles, J. "Dynamics of nonholonomic mechanical systems using a natural orthogonal complement", *ASME Journal of Applied Mechanics*, **58**, pp 238-244 (March 1991)

27. Craig, J., *Introduction to Robotics, Mechanics and Control*, Addison Wesley, Reading, MA, USA (1989).